

# Fish Bone

*by* Fahma Riyanti

---

**Submission date:** 27-Apr-2023 09:10AM (UTC+0700)

**Submission ID:** 2076718640

**File name:** ijfac\_fish\_bond\_2022.pdf (425.3K)

**Word count:** 3845

**Character count:** 19765

## Fixed-Bed Column for the Removal of Cd(II) from Aqueous by Hydroxyapatite from Red Snapper (*Lutjanus campechanus*) Fish Bone

Widia Purwaningrum<sup>1,2</sup>, Fahma Riyanti<sup>1,2,\*</sup>, Muhammad Said<sup>1,2</sup>, Poedji Loekitowati Hariani<sup>1,2</sup>, Aria Septi Handayani<sup>1</sup>

<sup>1</sup>Department of Chemistry, Faculty of Mathematics and Natural Sciences, Universitas Sriwijaya, Ogan Ilir 30662, Indonesia

<sup>2</sup>Research Centre of Advanced Material and Nanocomposite, Faculty of Mathematics and Natural Sciences, Universitas Sriwijaya, Ogan Ilir 30662, Indonesia

\*Corresponding Author: [fatechfj@unsri.ac.id](mailto:fatechfj@unsri.ac.id)

### Abstract

The Synthesis of hydroxyapatite from Red Snapper (*Lutjanus campechanus*) fish bone carried out. Hydroxyapatite is utilized for Cd(II) sorption from solution using a fixed-bed column. Hydroxyapatite was characterized using X-ray Diffraction, Fourier Transform Infra-Red, Scanning Electron Microscope-Electron Dispersive, and Thermogravimetric. In fixed-bed column, the influence of bed height (5, 10, 15 cm) and flow rate (6, 8 and 10 mL/min) were studied. The highest adsorption capacity is obtained at a bed height of 15 cm, and a flow rate of 6 mL/min with adsorption capacity is 47.027 mg/g. The predicted by Bed Depth Service Time (BDST) model obtained that value of  $R^2$  in the range 0.9964-0.9997. The adsorption capacity per unit volume ( $N_0$ ) is in the range 141.12-222.89 mg/L while  $k_a$  is in the range 0.0136-0.022 L/mg h. This indicates that BDST can be used to explain the performance of Cd(II) sorption onto hydroxyapatite by fix bed column.

**Keywords:** hydroxyapatite, fish bone, fixed-bed column, Cd(II)

### Abstrak (Indonesian)

Sintesis hidrosiapatit dari tulang ikan kakap merah (*Lutjanus campechanus*) telah dilakukan. Hidrosiapatit yang dihasilkan digunakan untuk mengadsorpsi ion Cd(II) menggunakan *fix bed column*. Karakterisasi hidrosiapatit yang dihasilkan menggunakan *X-ray Diffraction*, *Fourier Transform Infra-Red*, *Scanning Electron Microscope-Electron Dispersive*, dan *Thermogravimetric*. Pada penelitian ini dipelajari pengaruh tinggi kolom (5, 10, 15 cm) dan kecepatan alir (6, 8 and 10 mL/min). Kapasitas adsorpsi terbesar diperoleh pada tinggi kolom 15 cm, dan kecepatan alir 6 mL/min dengan kapasitas adsorpsi 47,027 mg/g. Berdasarkan prediksi *Bed Depth Service Time* (BDST) model diperoleh nilai  $R^2$  pada range 0,9964-0,9997. Kapasitas adsorpsi per unit volum ( $N_0$ ) pada range 141,12-222,89 mg/L, sedangkan nilai  $k_a$  pada range 0,0136-0,022 L/mg. Hasil ini mengindikasikan bahwa BDST dapat digunakan untuk menggambarkan adsorpsi Cd(II) pada hidrosiapatit menggunakan metode *fixed-bed column*.

**Kata Kunci:** hidrosiapatit, tulang ikan, *fixed-bed column*, Cd(II)

### Article Info

Received 15 April 2021  
Received in revised 27 May 2021  
Accepted 28 May 2021  
Available online 20 June 2021

### INTRODUCTION

Some heavy metals are important elements in life, as examples are needed for the human metabolic system. Other heavy metals are very toxic in trace levels and harmful to humans and the environment. [1,2]. Cadmium is one of the heavy metals produced naturally and from industrial processes such as electroplating, plastics, battery production, metallurgy, pigments, fertilizers, pesticides, textiles [2,3,4]. Cadmium is carcinogenic, and it can also cause

respiratory irritation, anemia, trachea bronchitis, pulmonary edema, kidney [1,2]. According to WHO, the concentration of cadmium in drinking water allowed a maximum of 0,005 mg/L [5].

Research to reduce heavy metals in the water is an important concern to obtain an effective and low-cost method. Various methods can be used to reduce cadmium in solutions such as coagulation, flocculation [6], ion exchange [7], ultrafiltration [8], chemical precipitation [9], deionization super capacitors [4], and

adsorption [2]. The adsorption method is a conventional method which is often used to reduce heavy metal ions because it is effective, simple and inexpensive [1,10,11]. The current study requires the development of bio sorbents from low cost material, abundantly available and have a large adsorption capacity.

Hydroxyapatite ( $\text{Ca}_{10}(\text{PO}_4)_6(\text{OH})_2$ ) is a bio sorbent that can be synthesized from biomaterials containing calcium such as mammalian bones, shell sources (eggs shells, stoves), marine sources (fish bones, fish scale) [12]. Hydroxyapatite has the potential as a bio sorbent for heavy metal because it has low water solubility, high stability against oxidation or reduction conditions and a large adsorption capacity [13]. Several researchers reported that have used hydroxyapatite for the adsorption process with batch methods including hydroxyapatite from eggshell to removal Pb(II) [14], synthetic hydroxyapatite for fluoride ion adsorption [15] and synthetic hydroxyapatite to reduce Zn(II) [13]. Fish bones are the most solid waste from fish consumption. Synthesis of hydroxyapatite from fish bone has economic and environmental value, that is low cost and reduces solid waste. Red snapper (*Lutjanus campechanus*) is one of the fish that has high economic value. In Indonesia, these fish are called kakap merah. This fish is generally consumed fresh, and most of it is exported in the form of fillets.

In this study, hydroxyapatite was extracted from red snapper fish bones by the heat treatment method. This method is considered the simplest, cheap and the most successful synthesis [16,17]. Sunil and Jaganathan [16] reported that the extraction of hydroxyapatite from roho labio fish bones at calcination temperatures of 600-1000 °C, obtained with high purity hydroxyapatite at temperature of 1000 °C with Ca/P ratio of 1.67. Hydroxyapatite produced is used to reduce Cd(II) using a fixed-bed column. This method is very suitable for treatment large-scale wastewater. This advantages of fixed-bed column compared to the batch experimental that is easy to operate, high adsorption capacity, can easily be converted from a laboratory scale, the volume of waste in large quantities can continuously flow. If the column is saturated, desorption can be done [11,18]. In this study, the effects of flow rate and bed depth are examined.

## MATERIALS AND METHODS

### Materials

Red snapper fish is obtained from traditional markets in Lubuk Linggau, South Sumatra. The

chemicals used are acetone,  $\text{CdCl}_2$ , ethanol, HCl, NaOH,  $\text{H}_3\text{PO}_4$  from Merck (Germany).

### Methods

#### Extraction of hydroxyapatite

The fish bones are boiled with water at 100 °C for 2 hours to remove salt, fish meat, and some impurities. Then, fish bones soaked with acetone. The fish bones cleaned using distilled water, then dried at room temperature for 24 h. The samples were crushed and grinded. Then, fish bone calcined in furnace at 750°C at heating rate 10°C/min for 5 hours to transform CaO. The hydroxyapatite preparation by adding  $\text{H}_3\text{PO}_4$  to fish bone powder with a molar ratio of Ca/P = 3: 2. The mixture was refluxed for 1 hour. The hydroxyapatite dried at temperature 100 °C for 1 hour.

#### Characterization of Hydroxyapatite

The crystallinity and crystallite size of hydroxyapatite were analyzed using X-Ray Diffraction (XRD Rigaku Miniflex 600). Data was obtained in  $2\theta$  in the range 10-80° using interval of 0.02°. The diffraction peak of hydroxyapatite compared with JCPDS (09-0432). The crystallite size ( $d$ ) is measure by the Debye-Scherrer equation:

$$d = \frac{0,9 \lambda}{\beta \cos(\theta)} \quad (1)$$

where  $\lambda$  is wavelength of Cu K $\alpha$  radiation source (1.5418 Å),  $\beta$  is the FWHM (full width at half maximum) intensity (rad), and  $\theta$  is the diffraction angle from Bragg's law (°).

Fourier Transform Infra-Red (FTIR Thermo Fisher Scientific) used for analyzed the functional group of hydroxyapatite. The transmittance (%) were determined in the wavenumber of 400-4000  $\text{cm}^{-1}$ . For surface morphology and element composition of hydroxyapatite were determined using a Scanning Electron Microscope-Energy Dispersive X-Ray Spectroscopy (SEM-EDS JEOL JSM) instruments.

#### Column adsorption

The Cd adsorption study using hydroxyapatite with the fixed-bed column method was carried out by glass column with diameter of 1.8 cm and a height of 50 cm. Bed height varies from 5, 10, and 15 cm while the flow rate is 6, 8 and 10 mL/min. The initial concentration of Cd(II) of 50 mg/L with pH solution of 6.0 (by addition of NaOH or HCl 0.1 M). The bottom of the column is equipped with glass wool. Peristaltic pumps are used to drain liquid sample ions in the column. Hydroxyapatite is poured into the column. Before the start operation, in the column flowed with deionized water in a downward flow to attract air

trapped between the particles. Figure 1 shows the schema of the column in the research.

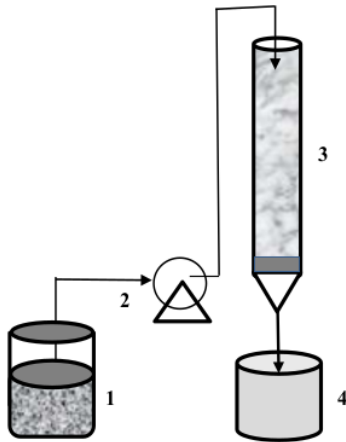


**Figure 1.** Schematic fixed-bed column of the laboratory scale. (1) Feed storage, (2) Peristaltic pump, (3) Glass column, (4) Effluent tank

#### Data analysis

Breakthrough curves are an important characteristic of operations using fixed-bed columns. When the eluent concentration has reached about 5%, it is the initial value of the points on the S shape curve that indicate the breakthrough point [19]. The total mass of Cd adsorbed was calculated using

$$q_{\text{total}} = \frac{Q_A}{1000} = \frac{Q}{1000} \int_{t=0}^{t=\text{total}} C_{\text{ad}} dt \quad (2)$$

Where  $q_{\text{total}}$  = total mass of Cd adsorbed (mg),  $Q$  = is flow rate,  $A$  is the area on the breakthrough curve,  $t$  is total time to flow (min), and  $C_{\text{ad}}$  is the Cd concentration of adsorbed (mg/L). Total amount of Cd in the column is calculated from:

$$m_{\text{total}} = \frac{C_0 Q t_{\text{total}}}{1000} \quad (3)$$

$C_0$  is initial concentration (mg/L), Capacity adsorption (mg/g) of hydroxyapatite at equilibrium time can be calculated from:

$$q_{\text{eq}} = \frac{q_{\text{total}}}{m} \quad (4)$$

$m$  is a weight of hydroxyapatite (dry) in the column. Effluent volume (mL) is calculated following:

$$V_{\text{eff}} = Q t_{\text{total}} \quad (5)$$

## RESULTS AND DISCUSSION

### Characterization of Hydroxyapatite

Figure 2 shows the XRD spectra of hydroxyapatite product synthesized by the heat treatment method. Identify the peak of hydroxyapatite by comparing with the XRD standard (JCPDS 09-0432). The  $2\theta$  of hydroxyapatite produced according to JCPDS are at 25.88 (002), 31.77 (211), 32.16 (112), 32.88 (300), 34.08 (202), 38.80 (310), 46.78 (222), 49.46 (213), 50.30 (321) and 53.10° (004). The strong diffraction peak at  $2\theta=31.74$ , indicated the purity of the hydroxyapatite synthesized. The particle size calculation using the Debye-Scherrer equation based on the peak at  $2\theta=31.77$  shows that the hydroxyapatite has a crystallite size of 34.50 nm. The crystallite size obtained in this study is similar to the crystallite size of hydroxyapatite from the bones of *Pangasius Hypothalmus* fish in the range 24.16-45.68 nm [20].

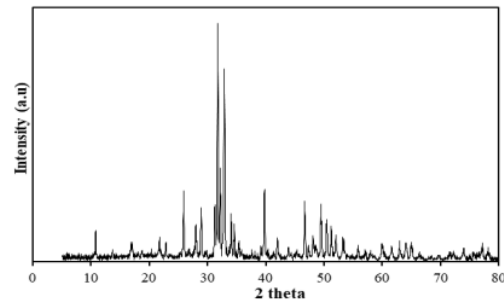


**Figure 2.** XRD pattern of hydroxyapatite

The characteristics of hydroxyapatite functional groups are shown in Figure 3. The IR band showing the presence of  $\text{PO}_4^{3-}$  Groups appear at wavenumbers 553-597, 987.42 and strong bands at 1020.02-1083.84  $\text{cm}^{-1}$ . The widening peaks at wave numbers 3100-3400 indicate absorbed water [21]. The peaks at 3567.81 and 626.78  $\text{cm}^{-1}$  indicate the stretching OH and in-plane bending from hydroxyapatite. Lugo et al [22] obtained the hydroxyl group of hydroxyapatite at a similar wave number of 3570 and 629  $\text{cm}^{-1}$ . The band at 1384.98  $\text{cm}^{-1}$  indicate the presence of carbonate groups. This study same with other studies on wave numbers 1384  $\text{cm}^{-1}$  [23].



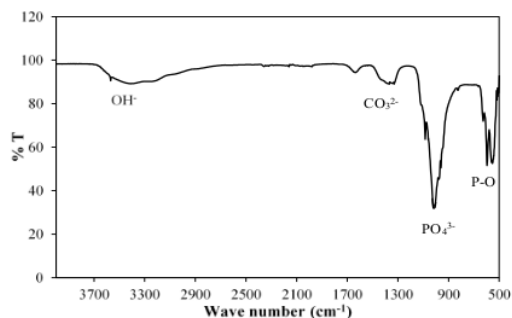


**Figure 3.** FTIR spectra of hydroxyapatite

The photograph of hydroxyapatite prepared from fish bones appear globular shape shown in Figure 4. In addition, it also appears the presence of pores. The composition of the elements of hydroxyapatite is expressed in table 1. The main components of the hydroxyapatite are Ca, O and P. This shows the purity of hydroxyapatite.

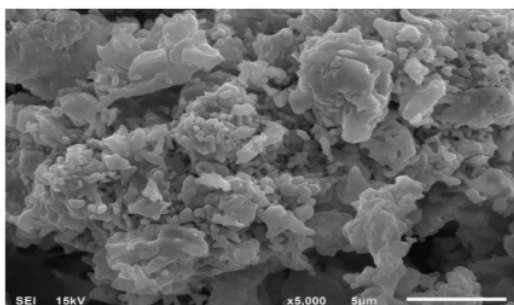


**Figure 4.** SEM photograph of hydroxyapatite

**Table 1.** Hydroxyapatite elements

Elements	Percentage (%)
O	46.07
P	16.73
Ca	36.20

Figure 5 illustrated the Thermogravimetric analysis of hydroxyapatite. At temperature 200 °C, a significant weight reduction from the absorbed water molecule adsorbed onto hydroxyapatite powder. The weight loss at this temperature is 5.2%. Furthermore, an increase in temperature causes the decomposition of hydroxyapatite. Deflection of temperature appears at a 450 °C from of small amount of organic matter present in hydroxyapatite. Spectra TG of hydroxyapatite from salmon appeared to be deflected at 465 °C [24]. The loss of weight from a temperature of 450-1000 °C is very small, less than 3%.

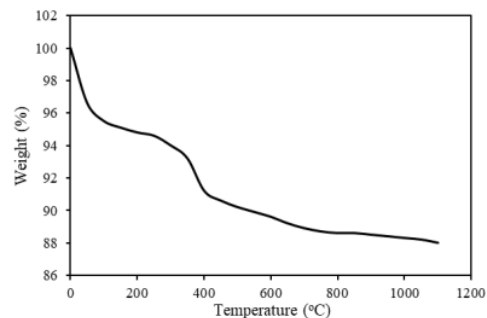


**Figure 5.** TG analysis of hydroxyapatite

#### *The effect of experimental condition*

Bed depth is one of the important parameters in the adsorption process using columns. In this study, the initial concentration of Cd(II) was 50 mg/L, and the flow rate was 6 mL/min with a bed depth of 5, 10 and 15 cm. Figure 6 shows the performance of the bed depths curve at different bed heights. The figure illustrates that breakthrough time increases with increasing bed height. The higher the bed height, the more amount of adsorbent, the increase in the surface area of adsorbent and the more active site of the adsorbent to adsorb Cd(II). Besides, the bed height increases, the lower the slope. The breakthrough with 5 cm bed height is saturated faster than other bed heights. According to Oguz [11], the phenomenon occurs because saturation in the binding sites is faster.

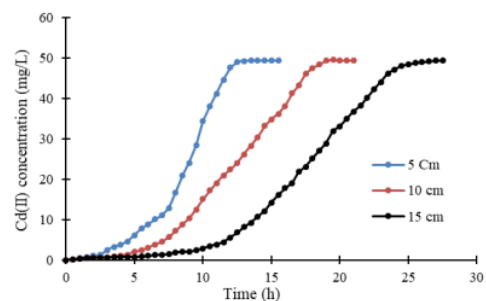


**Figure 6.** Breakthrough curves for adsorption of Cd(II)

Figure 6 shows the breakthrough curve at various flow rates, 6, 8, and 10 mL/min and bed height. The initial concentration of Cd used was 50 mg/L, and solution pH 6. The figures of different flow rate have the same pattern where columns with large flow rates have steeper graphs, indicated the effects of intra-particle diffusion. Maximum adsorption capacity is faster achieved in columns with large flow rates because more Cd(II) exchanges with functional groups of adsorbent in short time [25]. The mechanism of

adsorption of metal ions onto hydroxyapatite reported through two stages, namely the first stage of metal ions adsorbed on the surface of the POH group, then the ion exchange between metal ions ( $M^{2+}$ ) by Ca(II), in the following reaction [26].

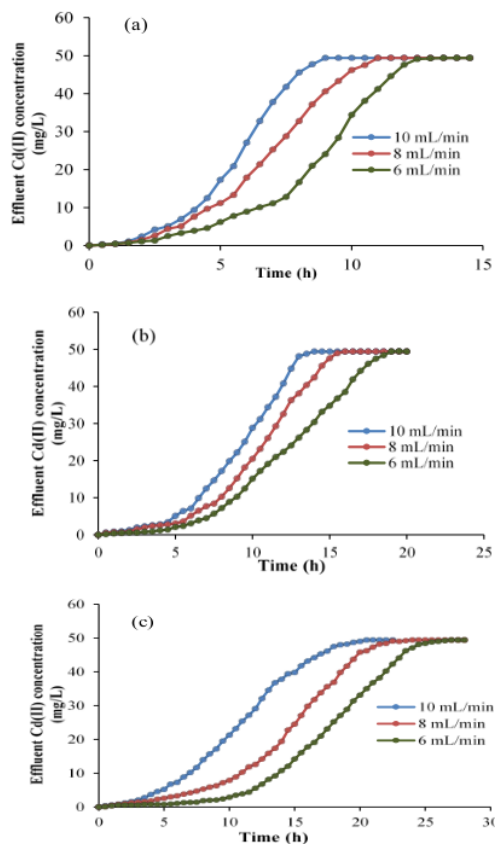
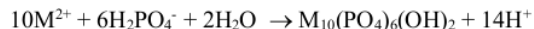
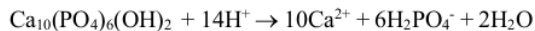


**Figure 7.** Breakthrough curves at bed height (a) 5 cm, (b) 10 cm and (c) 15 cm

Table 2 shows the parameters in the fixed-bed column. Increasing bed height increases adsorption capacity, and conversely increases flow rate, adsorption capacity decreases. The biggest adsorption capacity is at bed height 15 cm with a flow rate of 6 mL/min. This value depends on the total Cd(II) that pass through the column and the amount of mass of the adsorbent in the column.

**Table 2.** The parameter in the fixed-bed column

Bed height (cm)	Flow rate (mL/min)	$t_b$ (h)	$t_e$ (h)	$q_{eq}$ (mg/g)
5	6	2.1	12.5	21.74
	8	1.5	11.0	11.12
	10	1.2	9.0	7.48
10	6	3.8	19.0	33.09
	8	3.5	16.0	16.20
	10	2.8	14.0	12.16
15	6	5.6	27.0	47.03
	8	5.2	24.0	24.30
	10	4.1	20.5	17.07

Breakthrough modeling curves are very important for describing and analyzing adsorption-scale labs using columns for applications in industry. In this study, Bohard Adams model applied to predict behavior of the adsorption process. The BDST (Bed Depth Service Time) model is a development of the Bohard Adam model, which shows the relationship between bed height and operating time. This theory is based on reactions on the surface of the adsorbent. The equation is as follows:

$$t_b = \frac{N_o}{C_o V} \cdot Z - \frac{1}{k_a C_o} \ln \left( \frac{C_o}{C_b} - 1 \right) \quad (6)$$

Where  $t_b$  (h) is flow time,  $C_o$  and  $C_b$  are initial concentration and final concentration effluent,  $Z$  is bed height (cm),  $N_o$  is adsorption capacity and  $k_a$  is rate constant can be obtained from the slope and intercept of the linear plot  $t_b$  versus  $Z$ . Bohart Adams parameters using linear regression are shown in table 3. From the table, it clear that the value of  $k_a$  and  $N_o$  depends on the flow rate [25], the increase in flow rate also increases the kinetics constant and the reverse value of  $N_o$  decreases. This phenomenon shows that sorption kinetic has a contribution to mass transfer in the column system [19].

**Table 3.** Parameter of BDST adsorption of Cd(II) onto hydroxyapatite

Flow rate (mL/min)	$N_o$ (mg/L)	$k_a$ (L/mg h)	$R^2$
6	222.89	0.0136	0.9997
8	146.88	0.0151	0.9978
10	141.12	0.0227	0.9964

## CONCLUSION

This research has successfully synthesized hydroxyapatite from a fish bone by sonochemical

method. The hydroxyapatite obtained was 10 nm in size with a molar ratio of 1.68. Hydroxyapatite is effective for removal Cd(II) by fixed-bed column. The bed height and flow rate affect the adsorption capacity. Increasing bed height and decreasing flow rate provide good adsorption performance. The largest adsorption capacity is obtained at a bed height of 15 cm with a flow rate of 6 mL/min.

#### ACKNOWLEDGMENT

The research received funding from This research was funded by Hibah Kompetitif Universitas Sriwijaya for the 2020, No.0179.057/UN9/SB3.LPPM.PT/2020.

#### REFERENCES

- [1] R.A.K Rao and M. Kashifuddin. "Adsorption studies of Cd(II) on ball clay: comparison with other natural clays." *Arabian Journal of Chemistry*, vol. 9, No. 2, pp. S1233–S1241, 2016.
- [2] H. Javadian, F. Ghorbani, H. Tayebi, S.H. Asl, "Study of the adsorption of Cd (II) from aqueous solution using zeolite-based geopolymer, synthesized from coal fly ash; kinetic, isotherm and thermodynamic studies." *Arabian Journal of Chemistry*, vol. 8, pp. 837–849, 2015.
- [3] E. Elkhatib, A. Mahdy, F. Sherif, W. Elshemy. "Competitive adsorption of cadmium (ii) from aqueous solutions onto nanoparticles of water treatment residual." *Journal of Nanomaterials*, vol. 2016, pp. 1–10, 2016.
- [4] Q. Peng, L. Liu, Y. Luo, Y., Zhang, W. Tan, F. Liu, F.L. Suib, G. Qiu. "Cadmium removal from aqueous solution by deionization supercapacitor with birnessite electrode." *ACS Applied Materials & Interfaces*, vol. 8, no. 50, pp. 34405–34413, 2016.
- [5] D. Mohan, K.P. Singh, V.K. Singh. "Trivalent chromium removal from wastewater using low cost activated carbon fabric cloth." *Journal of Hazardous Materials*, vol. 153, pp. 280–295, 2006.
- [6] O.S. Amuda, I.A. Amoo, K.O. Ipinmoroti, O.O., Ajayi. "Coagulation/flocculation process in the removal of trace metals present in industrial wastewater." *Journal of Applied Sciences and Environmental Management*, vol. 10, no. 3, pp. 159–162, 2006.
- [7] Y. Bai, B. Bartkiewicz. "Removal of cadmium from wastewater using ion exchange resin amberjet 1200H columns." *Polish Journal of Environmental Studies*, vol. 18, no. 6, pp. 1191–1195, 2009.
- [8] D.J. Ennigrou, L. Gzara, M.R.B. Romdhane, M. Dhahbi. "Cadmium removal from aqueous solutions by polyelectrolyte enhance ultrafiltration." *Desalination*, vol. 246 (1-3), pp. 42–48, 2009.
- [9] M. Byambaa, E. Dologor, K. Shiomori, Y. Suzuki. "Removal and recovery of heavy metals from industrial wastewater by precipitation and foam separation using lime and casein." *Journal of Environmental Science and Technology*, vol. 11, No. 1, pp. 1–9, 2018.
- [10] Z. Xue, N. Liu, H. Hu, J. Huang, Y.K. Kalkhajaeh, X. Wu, N. Xu, X. Fu, L. Zhan. "Adsorption of Cd(II) in water by mesoporous ceramic functional nanomaterials." *Royal Society Open Science*, vol. 6, pp. 1–11, 2019.
- [11] E. Oguz. "Fixed-bed column on the removal of Fe<sup>3+</sup> and neural network modelling." *Arabian Journal of Chemistry*, vol. 10, pp. 313–320, 2017.
- [12] N.A.S.M. Pu'ad, P. Koshy, H. Z. Abdullah, M.I. Idris, T.C. Lee. "Syntheses of hydroxyapatite from natural sources." *Heliyon*, vol. 5, No. 5, pp. 1–14, 2019.
- [13] E. Skwarek, A.G. Palaska, J.B. Choromanska, E. Broda. "Adsorption of uranium ions on nano-hydroxyapatite and modified by Ca and Ag ions." *Adsorption*, vol. 25, pp.639–647, 2019.
- [14] A.R. Ibrahim, Y. Zhou, X. Li, L. Chen, Y. Hong, Y. Su, H. Wang, J. Li. "Synthesis of rod like hydroxyapatite with high surface area and pore volume from eggshell for effective adsorption of aqueous Pb(II)." *Materials Research Bulletin*, vol. 62, pp. 132–141, 2015.
- [15] M. Mourabet, A.El. Rhilassi, H. El. Boujaady, M.B. Ziatni, R.El. Hamri, A. Taitai. "Removal of fluoride from aqueous solution by adsorption on hydroxyapatite (Hap) using response surface methodology." *Journal of Saudi Chemical Society*, vol. 19, No. 6, pp. 603–615, 2015.
- [16] B.R. Sunil, and M. Jaganathan. "Producing hydroxyapatite from fish bone by heat treatment." *Materials Letters*, vol. 185, pp. 411–414, 2016.
- [17] M. Boutinguinza, J. Pou, R. Comesana, F. Lusquinos, A. Carlos, B. Leon, "Biological hydroxyapatite obtained from fish bones", *Materials Science and Engineering: C*, 32, 478–486, 2012.
- [18] A. Kara, G.E. Ustun, S.K.A. Solmaz, E. Demirbel. "Removal of Pb(II) ions in fixed-bed column from electroplating wastewater of Bursa, an industrial city in Turkey." *Journal of Chemistry*, vol. 2013, pp.1–6, 2013.

- [19] S. Srivastava, S.B. Agrawal, M.K. Mondal. "Fixed bed column adsorption Cr(VI) from aqueous solution using nanosorbents derived from magnetite impregnated *Phaseolus vulgaris* Husk." *Environmental Progress & Sustainable Energy*, vol. 2018, pp. 1–9, 2018.
- [20] P.L. Hariani, and M. Said, Salni. "Effect sintering on the mechanical properties of hydroxyapatite from fish bone (*Pangasius Hypohtalmus*)." in *IOP Conference Series: Materials Science and Engineering*, 509, 1–9, 2019.
- [21] M. Mujahid, S. Sarfraz, S. Amin. "On the formation of hydroxyapatite nano crystals prepared using cationic surfactant", *Materials Research*, vol. 18, No. 3, pp. 468–472, 2015.
- [22] V.R. Lugo, T.V.K. Karthik, D.M. Anaya, E.R. Rosas, L.S.V. Ceron, M.I.R. Valderrama, E.S. Rodriguez. "Wet chemical synthesis of nanocrystalline hydroxyapatite falkes: effect of pH and sintering temperature on structural and morphological properties." *Royal Society Open Science*, vol. 5, pp. 1–14., 2018.
- [23] M. Manoj, D. Mangalaraj, N. Ponpandian, C. Viswanathan. "Core shell hydroxyapatite/Mg nanostructure: surfactant free facile synthesis, characterization and their in-vitro cell viability studies against leukemia cancer cells (K562)." *RSC Advances*, vol. 5, pp. 48705–48711. 2015.
- [24] J. Venkatesan, B. Lowe, P. Manivasagan, K. Kang, E.P. Chalisserry, S. Anil, DG. Kim, S. Kim. "Isolation and characterization of nano-hydroxyapatite from salmon fish bone." *Materials*, vol. 8, pp. 5426–5439, 2015.
- [25] C. Yunnen, W. Ye, L. Chen, G. Lin, N. Jinxia, R. Rushan. "Continuous fixed-bed column study and adsorption modeling: removal of arsenate and arsenite in aqueous solution by organic modified spent grains." *Polish Journal of Environmental Studies*, vol. 26, No. 4, pp. 1847–1854, 2017.
- [26] I. Mobasherpour, E. Salahi, M. Pazouki. "Comparative of the removal of  $Pb^{2+}$ ,  $Cd^{2+}$  and  $Ni^{2+}$  by nano crystallite hydroxyapatite from aqueous solutions: adsorption isotherm study." *Arabian Journal of Chemistry*, vol. 5, pp. 439–446, 2012.



# Fish Bone

---

## ORIGINALITY REPORT

---

**18%**

SIMILARITY INDEX

**10%**

INTERNET SOURCES

**11%**

PUBLICATIONS

**6%**

STUDENT PAPERS

---

## MATCH ALL SOURCES (ONLY SELECTED SOURCE PRINTED)

---

1%

★ [citeseerx.ist.psu.edu](http://citeseerx.ist.psu.edu)

Internet Source

---

Exclude quotes      Off

Exclude matches      Off

Exclude bibliography      Off